Indian Journal of Pure & Applied Physics
Vol. 51, December 2013, pp. 860-863

Effect of gold electrode annealing on gas sensing properties of nano-and microstructures of macroporous silicon

S Sadr[1]*, M E Azim-Araghi[1], M Rahimi[1] & R S Dariani[2]

[1]Department of Physics, Kharazmi University, Tehran, Iran

[2]Department of Physics, Alzahra University, Tehran, Iran

*E-mail: so.sadr@ymail.com

Received 12 December 2012; revised 7 March 2013; accepted 9 October 2013

This paper presents porous silicon (PS) with nano-and microstructures as carbon dioxide sensing layers. The *p*-type Si substrate is subjected to PS etching. The PS morphology has been characterized by scanning electron microscope. According to the parameters of electrochemical process, PS layers were found to have a different structure. By using dimethylformamide (DMF) in electrolyte, regular, honeycomb-like and macroporous structures were formed. PS side of the substrate is then coated with a thin layer of gold and annealed at 500°C. These devices, which operate at room temperature, are more sensitive to the applied voltages in CO_2 gas. The effect of annealing of gold electrode on current-voltage and response-voltage characteristics of PS has been studied. Our results show that the conductivity and response of PS sensors improve much more when its surface is modified with annealing of gold electrode and also nanostructured PS has greater response than the others.

Keywords: Porous silicon, Nano-and microstructure, Macroporous, Conductivity

1 Introduction

The development of solid-state sensors with high sensitivity to gas adsorption especially at lower operating temperatures is an important problem[1-3]. In recent years, a great attention has been paid to the development and application of environmental gas sensors[4]. Porous silicon (PS), obtained conventionally by anodization of crystalline *p*-type silicon, is a potential platform for high efficiency gas sensors mainly due to its very large surface to volume ratio, which enhances adsorption of the sensing gas, a primary step for gas sensor[5]. Nanostructured PS has been investigated for applications as diverse as optic[6-8], chemical sensor[9-11], tissue engineering[12], cell culture[13], drug delivery[14], biotechnology, gas separation and microelectronics[15]. Series applications of PS in sensor technology have been based on change of conductivity or capacity of material upon adsorption of gas molecules[16]. The gas detection can be carried out to a wide range of physical, chemical, electrochemical and optical principles[17]. Advantages of PS sensors are low cost, room temperature operation and possible integration with electronic circuits[18].

In the present paper, we focus on the fabrication of nano-and microstructured macroporous silicon. The electrical behaviour and sensing properties in exposing to the CO_2 gas with and without annealing treatment of gold electrode on the PS surface have been investigating.

2 Experimental Details

The PS samples were fabricated by anodization of *p*-type silicon wafer. This initial material was a single crystalline silicon wafer with (100) orientation, B-doped, thickness 525 μm having resistivity between 1 and 5 Ω cm. The starting silicon was finished single side polished (SSP) and other side was etched.

Before anodization, the native oxide was removed from the rear side of the wafer in aqueous solution (30% KOH), and ohmic contact was deposited by thermal evaporation of a thin aluminium layer followed by vacuum annealing process at 450°C for 30 min in a furnace. The PS layers were formed by electrochemical anodization using a mixture of 38-40% concentrated hydrofluoric acid (HF) and DMF as electrolyte. The anodized wafer and platinum cathode were kept parallel to each other with a distance of 1 cm between them in electrochemical cell to form homogeneity porous layers. The current was flowed to the polished surface of wafer. The etching was done at room temperature. The current densities were 15 and 35 mA/cm^2 with the same anodization time of 20 min. The ratio concentration of electrolytes was

HF: DMF; 1:4 and 1:3 by volume. After formation, PS samples were rinsed in 10% HF solution for 5 s to remove the native oxide layer and dipped into distilled water and allowed to dry in ambient air. Porous structures were investigated by scanning electron microscope (SEM). Average value of the width of pores was defined as arithmetical mean of 10 different pores (measured at the half depth of pore), i.e.: $d=\sum d_i/n$, where $n=10$. Measurements of d_i were performed by SEM[19] and also in the same way the average value of the width of pores walls was calculated.

Gold electrode was evaporated on the PS side of the substrate and then this thin film was stabilized on the PS surface through an annealing. The samples were placed inside an electric oven and annealed at 500°C for 10 min. Thin copper wires were connected to the gold electrodes using silver paste for electrical measurements. For the electrical characterization, the samples were kept in a small sealed chamber with inlet and outlet provisions for gases. The pressure of CO_2 gas in the chamber was 20 sccm. Sensing properties of the device towards CO_2 gas at room temperature and ambient pressure have been studied. These properties have been compared before and after CO_2 exposure for samples with and without annealing treatment of gold electrode.

3 Results and Discussion

Figure 1 shows that nano-and microstructured PS were obtained by using DMF in electrolyte, which caused to form regular structures and also macroporous layers, whose pore sizes are larger than 50 nm. The dependence of the pores and their walls width on current density can be observed in Fig. 1(a and b). In both, PS layers were grown at different current density range, but the HF concentration was held constant.

It can be seen that the average pores' width increases as current density increases and forms a honeycomb-like structure. It is important to note, that at high current density (35 mA/cm^2) the inter-pore spacing decreases and consist of network of silicon nanocrystals with average value of 91 nm due to large width of the pores. It was concluded that the increasing of the current density from 15 mA/cm^2 to 35 mA/cm^2 change the average value of the pores width from 441 nm to 806 nm and a change of the residual structure from microstructure to nanostructure.

In Fig. 1(b and c), the concentration of DMF is different for each PS sample, but the other parameters are kept the same. It can be clearly seen from Fig. 1(b and c) that increasing the concentration of DMF in the electrolyte increases the average value of the pores width.

Meanwhile, according to SEM images, a change of the electrolyte ratio from HF: DMF; 1:4 to 1:3 leads to increasing of the average width of pores walls from 210 nm to 263 nm.

To have a better comparison of PS skeleton in Fig. 1(d-f), the SEM images of samples are shown at

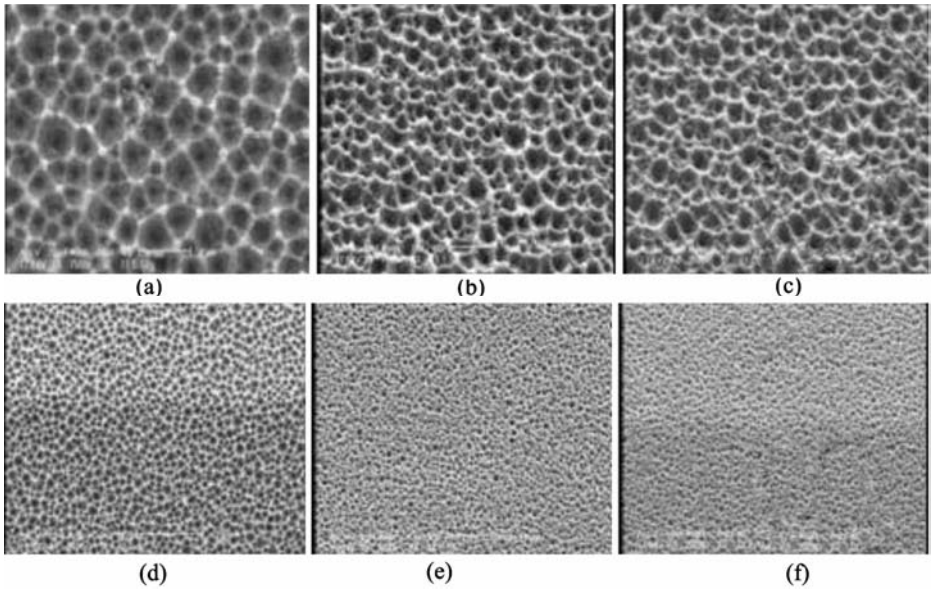

Fig. 1 — SEM images (scale bar 2 µm) (a) top view of S_1 (b), (c) "bird eye's view" of S_2, S_3 respectively and SEM images (scale bar 10 µm) (d) top view of S_1 (e), (f) "bird eye's view" of S_2, S_3 respectively

Table 1 — Specific features of the studied PS layer

Sample	Anodization time (min)	Current density (mA/cm^2)	Electrolyte ratio (HF:DMF)	Average width of pores (nm)	Average width of pores walls (nm)
S_1	20	35	1:4	806	91
S_2	20	15	1:4	441	210
S_3	20	15	1:3	362	263

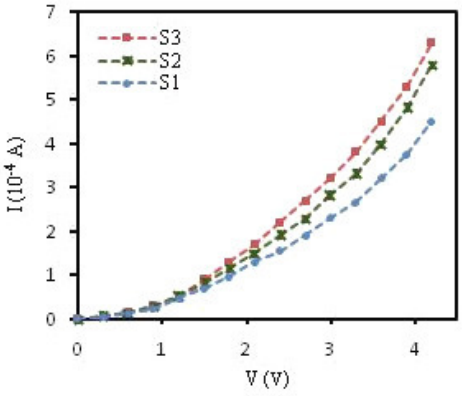

Fig. 2 — Current-voltage characteristics of Au/PS/Si /Al structure in air at room temperature

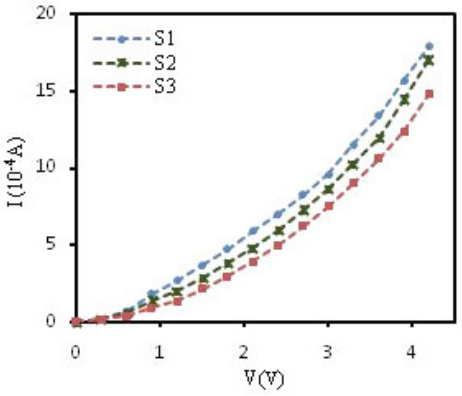

Fig. 3 — Current-voltage characteristics of Au/PS/Si /Al structure after CO_2 exposure at room temperature

scale bar 10 µm. The dependence of the pores and their walls width on anodization parameters is summarized in Table 1.

The characteristic I-V curves corresponding to PS samples in ambient air at room temperature are shown in Fig. 2.

Figure 2 shows that with increasing average width of pores and decreasing their walls, conductivity of PS samples is reduced (Table 1) which is due to an increase in surface resistivity. Therefore, the nanostructured PS exhibit weak conductivity in air.

The I-V characteristics as shown in Fig. 3, have been measured for CO_2 gas at room temperature. The flow of 20 sccm gas over the surface of the device

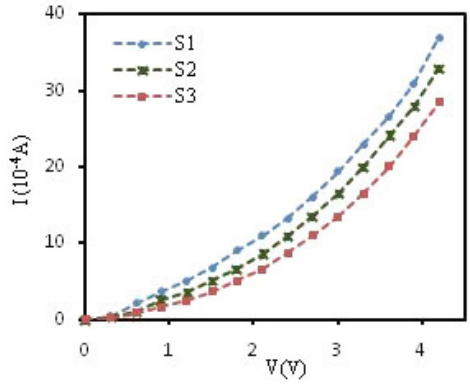

Fig. 4 — Current-voltage characteristics of Au/PS/Si /Al structure with gold electrode annealing after CO_2 exposure at room temperature

causes the conductivity to change and it is readily monitored.

After applying the CO_2 gas, a continuous increase in the conductivity was observed for entire applied voltage range in all samples. It can be seen in Fig. 3, a large current variation is observed for sample S_1 as compared to other samples. There are several approaches to explain the variation of the current in the presence of gas. Activation of trapping centers due to adsorbate interaction with dangling bond states can explain conductance variations due to the trapping or release of carriers[20]. Furthermore, the molecules of CO_2 act as acceptor centers. Once they have been adsorbed on PS surface, the acceptor-like character would lead to an increase of free carrier (holes) concentration thus explaining the increase in conductivity[17].

The effect of gold electrode annealing on the Au/PS/Si/Al structure I-V characteristics can be seen in Fig. 4. Annealed devices were submitted to a test in a sealed chamber at 20 sccm. Fig. 4 shows when gold electrode annealed, the electrical properties of the Au/PS/Si/Al characteristics are improved because the Au/PS layer on the silicon surface without annealing is more surface resistivity and blocks free carrier at the interface of silicon and metal.

The relative response of the current ($\Delta I/I_a$) of the sensors is calculated, where ΔI is the difference between the current in air (I_a) and the current in

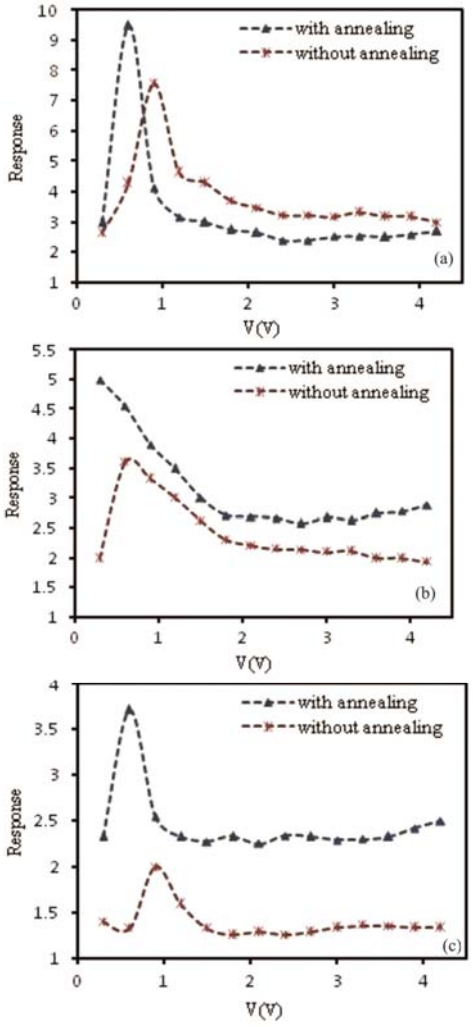

Fig. 5 — Response-voltage characteristics of Au/PS/Si /Al structure with and without gold electrode annealing after CO_2 exposure at room temperature for (a) S_1 (b) S_2 (c) S_3

Table 2 — Sensing parameters for PS sensors at room temperature

Au/PS/Si/Al	Biasing voltage (V)			Maximum response		
structure	S_1	S_2	S_3	S_1	S_2	S_3
Without annealing	0.9	0.6	0.9	7.57	3.61	2
With annealing	0.6	0.3	0.6	9.5	5	3.72

presence of CO_2 gas (I_g). Figure 5(a-c) shows the response-voltage characteristics of the samples with and without gold electrode annealing for CO_2 gas at room temperature. It reaches the maximum response for the nanostructure device (S_1). On the other hand, the microstructure samples were not as sensitive as the nanostructure one. It shows that the high sensitivity is observed for low applied voltage.

Table 2 presents the values of response and the voltage corresponding to maximum response of the samples with and without gold electrode annealing. The annealed samples exhibit more sensitivity to CO_2 than without annealing samples and it enhances the response due to an increasing in number of activated centers.

4 Conclusions

The present work contains the results of a study on the effect of the adsorption of the CO_2 on I-V characteristics of PS-based nano-and microstructures and the effect of annealing of gold electrode over the PS surface on conductivity and response of the devices. In the present case, various morphologies are formed depending on the anodization conditions.

It has been observed that sensors made with PS and annealed gold electrode demonstrate a significant increase in conductivity and response when exposed to CO_2. It was revealed that the response of the nanostructured sensor upon gas adsorption is visibly much improved as compared with the microstructured one. The values of the voltage corresponding to maximum response of these low-cost devices with gold electrode annealing are highly improved.

References

1 Lundstrom I, *Sensors & Actuators*, 1 (1981) 403.
2 Litovchenko V G, Gorbanyuk T I, Efremov A A *et al*, *Sens & Actuators*, 74 (1999) 233.
3 Litovchenko V G, Gorbanyuk T I, Efremov A A & Evtukh A A, *Microelectron Reliab*, 40 (2000) 821.
4 Waghuley S A, *Indian J Pure & Appl Phys*, 49 (2011) 816.
5 Kanungo J, Saha H, Basu S, *Sensors & Transducers*, 103(4) (2009) 102.
6 Lockwood D J, Wang A & Bryskiewicz B, *Solid State Commun*, 89(7) (1994) 587.
7 Weiss S M & Fauchet P M, *IEEE J Sel Top Quantum Electron*, 12(6) (2006) 1514.
8 Pavlikov A V, Lartsev A V, Gayduchenko I A & Timoshenko V Yu, *Microelectron Eng*, 90 (2012) 96.
9 Gelloz B, Sano H, Boukherroub R *et al*, *Appl Phys Lett*, 83(12) (2003) 2342.
10 Gabouze N, Belhousse S, Cheraga H *et al*, *Vacuum*, 80(9) (2006) 986.
11 Mahmoudi Be, Gabouze N, Haddadi M *et al*, *Sens & Actuators B*, 123 (2007) 680.
12 Alvarez S D, Derfus A M, Schwartz M P *et al*, *Biomaterials*, 30(1), (2009) 26.
13 Agrawal A A, Nehilla B J, Reisig K V *et al*, *Biomaterials*, 31(20) (2010) 5408.
14 Haidary S M, Corcoles E P & Ali N K, *J Nanomaterials*, 2012 (2012) 1.
15 Bogaerts W, de Heyn P, van Vaerenbergh T *et al*, *Laser & Photonics Rev*, 6(1) (2012) 47.
16 Dzhafarov T, *J Qafqaz Univ*, 25 (2009) 20.
17 Mahmoudi Be, Gabouze N, Haddadi M *et al*, *Phys Status Solidi (c)*, 4(6) (2007) 2068.
18 Pancheri L, Oton C J, Gaburro Z *et al*, *Sensors & Actuators B*, 89 (2003) 237.
19 Jarimaviciute-Zvalioniene R, Grigaliunas V, Tamulevicius S & Guobiene A, *Mater Sci*, 9(4) (2003) 317.
20 Bisi O, Ossicini S & Pavesi L, *Surf Sci Rep*, 38 (2000) 1.